

Disrupting Transcriptional Feedback Yields an Escape-Resistant Antiviral

Sonali Chaturvedi¹, Marie Wolf¹, Noam Vardi¹, Raghav Singhal², Ariel D. Weinberger², Matilda Chan^{3,4}, Leor Weinberger^{1,5,6*}

¹Gladstone|UCSF Center for Cell Circuitry, Gladstone Institutes, San Francisco, CA 94158;

²Autonomous Therapeutics Inc., New York, NY 10013

³Francis I. Proctor Foundation, University of California, San Francisco, San Francisco, CA 94122;

⁴Departments of Ophthalmology,

⁵Biochemistry and Biophysics, and

⁶Pharmaceutical Chemistry, University of California, San Francisco, CA 94158

*to whom correspondence should be addressed: leor.weinbeger@gladstone.ucsf.edu

Abbreviations: circuit disrupting oligonucleotide therapy (C-DOT); human cytomegalovirus (CMV); herpes simplex virus type 1 (HSV-1)

Keywords: herpesvirus; autoregulatory circuit; transcriptional feedback; viral evolution; oligonucleotide therapy

Abstract: 125 words

Main Text: 2140

Figures: 4 (color)

Abstract

Drug resistance is a substantial clinical problem, with combination therapies often the only recourse. Here, we propose a novel antiviral approach that disrupts viral auto-regulatory circuits, which limits resistance by requiring multiple viral mutations. We provide proof-of-concept that DNA-based circuit-disruptor oligonucleotide therapies (C-DOTs) interfere with transcriptional negative feedback in human herpesviruses (CMV and HSV-1) thereby increasing viral transcription factors to cytotoxic levels. C-DOTs reduce viral replication >100-fold, are effective in high-viremic conditions where existing antivirals are ineffective, and show efficacy in mice. Strikingly, no C-DOT-resistant mutants evolved in >60 days of culture, in contrast to approved herpesvirus antivirals where resistance rapidly evolved. Oligonucleotide therapies that target feedback circuits could mimic combination therapy and represent escape-resistant interventions with broad applicability to viruses, microbes, and neoplastic cells.

One Sentence Summary

A single oligonucleotide breaks transcriptional feedback and mimics combination therapy to limit the emergence of antiviral resistance.

From bacteria to cancers, drug resistance arising from ‘escape’ mutations causes substantial morbidity and mortality (1-3). The time to escape mutant arisal can be estimated from the mutation rate, μ , and the effective population size, N , (4, 5) and many viruses exhibit large μ such that frequency of mutants ($\mu \times N$) is >1 even for moderate virus population sizes (e.g., if $\mu \sim 10^{-5}$ then for $\mu \times N > 1$ only requires $N > 10^5$). Herpesviruses, for example, exhibit high mutation rates (6, 7), which may explain the substantial antiviral resistance observed in clinical settings (8, 9). In particular, herpes simplex virus type 1 (HSV-1)—a leading cause of blindness—exhibits resistance to acyclovir (ACV) in ~40% of transplant patients (10) while human herpesvirus 5, cytomegalovirus (CMV)—a leading cause of birth defects and transplant failure—exhibits resistance to ganciclovir (GCV) in 30–75% of patients (11). ACV and GCV resistance arises because their antiviral activity requires herpesvirus thymidine kinase (TK), and single-base mutations destroy TK activity with a $\mu \sim 10^{-3}$ (6) driving TK escape mutants within a single generation (12), which ultimately promoted the development of non-TK drug targets (13, 14). Resistance to these new therapies is still being clinically evaluated, but, given the generality of resistance to antimicrobials (1-3), is likely unavoidable.

Combination therapy, wherein multiple drugs simultaneously inhibit different viral targets, is one approach used to limit antiviral resistance. For a two-drug therapy, escape mutants are predicted to arise at a rate $\sim \mu^2$ (i.e., the requirement for mutants to arise becomes $\mu^2 \cdot N > 1$), which requires substantially larger virus populations (i.e., $N > \mu^{-2}$). However, each constituent antiviral must have a distinct molecular target, as well as favorable toxicity, efficacy, bioavailability, and dosing profiles. These criteria can be challenging to satisfy and such targets are still being characterized for herpesviruses. Conceptually, transcriptional auto-regulatory (feedback) circuits may present a combination-therapy target with unique properties (15). Both CMV and HSV-1 utilize transcriptional feedback to regulate immediate-early (IE) viral gene expression, which is obligate to transactivate downstream viral genes, ultimately licensing virus maturation (16-19). In CMV, the 86-kDa immediate early (IE86; a.k.a. IE2) protein, and in HSV-1 the IE175 (a.k.a. ICP4) protein, are indispensable transcriptional transactivators (20, 21). Critically, IE86 and IE175 are cytotoxic when expression is misregulated above tightly auto-regulated homeostatic levels, and both CMV and HSV-1 encode negative-feedback circuits to maintain IE86 and IE175 levels below their respective cytotoxic thresholds (20, 22). These feedback circuits are comprised of a protein-DNA interaction wherein the IE protein binds to a 14–15 bp palindromic cis-repression sequence (crs) within its respective promoter and auto-represses its own transcription (Fig. 1A). Disrupting this feedback by altering the crs increases IE protein levels to cytotoxic levels, leading to a >100 -fold reduction in viral replication (22, 23).

We hypothesized that oligonucleotides mimicking the palindromic DNA-binding site could titrate IE proteins away from the crs and act as competitive inhibitors to disrupt IE negative feedback (Fig. 1A). Mathematical modeling predicted that such circuit-disrupting oligonucleotide therapies (C-DOTs) may in fact raise IE protein to cytotoxic levels (Fig. 1B and fig. S1). Theoretically, to escape C-DOTs and recapitulate a feedback loop, the virus would need to evolve a new IE-protein domain to recognize a new DNA sequence and *simultaneously* evolve a new cognate DNA binding sequence in the IE promoter; these C-DOT escape mutants would evolve on order of μ^2 , which would occur substantially slower than observed for ACV/GCV resistance (Fig. 1C). It is conceivable that single mutants in the IE protein could arise and bind alternate crs-like sequences pre-existing in the promoter region, thereby circumventing the combinatorial mutation

hypothesis. However, there are no comparable palindromes within 500 bp of the MIEP promoter and if such sequences were present, then crs-deletion mutants should strongly select for such IE86 mutants that can recapitulate negative feedback, which does not occur over ~1 month of culturing (22).

To find oligonucleotides that optimally titrate IE proteins, we developed an *in vitro* liquid-chromatography assay to quantify the efficiency of various linear DNA oligonucleotides in catalyzing formation of the IE86 protein-DNA complex (Fig. 2A). To validate the assay, we used electrophoretic mobility shift assays (EMSA) and verified that purified IE86 protein bound double-stranded DNA oligonucleotides in a sequence-specific manner (fig. S2). We tested an array of crs-encoding oligonucleotides of various lengths and found a linear 28 base-pair (bp) DNA most efficiently catalyzed formation of the IE86-DNA complex (Fig. 2B–C). Shorter or longer crs-encoding DNAs were less efficient at titrating IE86 and promoting protein-DNA complex formation.

To test if these DNAs disrupted negative feedback, we used a retinal pigment epithelial cell line stably transduced with a previously described minimal IE86 negative-feedback reporter circuit (22). These cells express the IE86 and GFP under the control of the IE86 promoter-enhancer such that increases in GFP indicate disruption of negative-feedback leading to cell death 48–72 hours later (Fig. 2D). Cells were nucleofected with the putative C-DOTs, or sequence-scrambled control oligonucleotides, and GFP expression assayed by flow cytometry at 48 h (Fig. 2D). DNA uptake by cells was verified by cy3 fluorescence (fig. S3A) and to enhance oligonucleotide stability, DNAs were modified by internal phosphorothioate bonds (fig. S3B). In agreement with the biochemical assays, the 28bp DNA most efficiently increased the GFP+ population (Fig. 2E) and correspondingly decreased live-cell percentages (Fig. 2F). Feedback-circuit disruption was dose dependent (fig. S4) and was enhanced by concatemerization as well as using nanoparticles to enhance cell uptake (fig. S5). Collectively, these results indicated that relatively short (< 30bp) double-stranded DNAs might be viable circuit disruptor oligonucleotides.

Next, we investigated the effects of disrupting transcriptional feedback in the context of viral infection. We designated the 28bp DNA for CMV IE86 as C-DOT^C (C-DOT for CMV) and found that C-DOT^C efficiently disrupted IE86 negative feedback in cells infected with a clinically-derived isolate of CMV (24) (Fig. 3A). We next hypothesized that replacing the 14bp crs within C-DOT^C with the 15bp repression sequence from IE175's promoter could generate a C-DOT for HSV-1 (now termed C-DOT^H). As predicted, C-DOT^H disrupted IE175 negative feedback in cells infected with clinically-derived HSV-1 (25) (Fig. 3B). There was minimal difference in %IE positive cells, indicating that C-DOTs did not alter permissiveness of cells to viral infection (fig. S6). Strikingly, the C-DOTs also reduced single-round viral replication titers for both CMV and HSV-1 at multiplicity of infection (MOI) of 0.1 by ~100 fold (Fig. 3C–D), in agreement with genetic disruption of IE negative feedback (22). To be sure that the observed antiviral effects were not specific to the virus strain or cell type used, we also tested (i) CMV strain AD169 and (ii) various GCV-resistant CMV strains in human foreskin fibroblasts, as well as (iii) murine CMV and (iv) rhesus CMV, in mouse and primate cells respectively, and in all cases found similar 100-fold titer reduction using the corresponding C-DOTs (figs. S7–S8).

In stark contrast to ACV and GCV, C-DOT increases virus fold reduction at higher MOI, and, at MOI = 2, C-DOTs exhibited a > 1300x reduction whereas ACV/GCV elicited 35–70x reduction in viral replication (Fig. 3C–D). Such robustness to high-viremic conditions has not been previously described for an antiviral (26), but is consistent with the putative C-DOT mechanism of action through feedback disruption and IE-mediated cytotoxicity—higher MOIs deliver more genomes, which generates more potentially cytotoxic IE protein.

Importantly, sequence-scrambled oligonucleotides (C-DOT^{Scram}) did not exhibit antiviral effects suggesting that C-DOTs are not acting via innate-immune mechanisms (e.g., activation of cGAS-STING pathway via TLR9), which is consistent with efficient cGAS pathway activation requiring DNAs of > 300bp (27), whereas C-DOTs are < 30bp. However, to verify that C-DOT activity is independent of cGAS-STING, we tested C-DOTs under conditions of high and low cGAS-STING expression and observed little difference in C-DOT antiviral effects and no effects for C-DOT^{Scram} in either setting (fig. S9). Moreover, C-DOTs did not activate TLR9 expression (fig S10).

Next, to examine the rate of emergence of viral escape mutants, we used a continuous-culture approach where virus was consecutively passaged from infected cells to fresh uninfected cells every 4 days (a typical CMV replication round) until virus was undetectable in presence of C-DOT treatment (~40–60 days; Fig. 3E). C-DOT^C was compared to Fomivirsen (28), the first approved DNA oligonucleotide therapy (an anti-sense DNA for IE86); C-DOT^H was compared with ACV (fig. S11). As previously reported (12), we found HSV-1 resistance to ACV emerges within two rounds of infection (fig. S11C) and that CMV resistance to Fomivirsen (28) arises within 3–4 rounds of infection (fig. S11A–B).

In striking contrast, C-DOT^C steadily reduced CMV titers to below the limit of detection by day 52, with no evidence of CMV resistance to the C-DOT^C (Fig. 3F and fig. S12). Similarly, C-DOT^H steadily reduced HSV-1 titers to below detection by day 40, with no evidence of resistance (Fig. 3G). Subsequent sub-culturing indicated that virus was cleared and that pre-clearance C-DOTs were not altering the virus replicative phenotype as C-DOT removal caused a 100-fold increase in titer for all time points until clearance (fig. S13). In agreement with this, sequence analysis indicated that no virus mutations arose in the 500bp-region surrounding the promoter repression sequences (fig. S14) and only single-nucleotide transient polymorphisms in the IE-protein regions responsible for DNA binding (fig. S15). Overall, these results indicate that disrupting feedback may be an escape-resistant antiviral strategy.

Finally, we tested if transcriptional feedback could be disrupted *in vivo* using the established model of herpes infection in mice (29). Briefly, in this model, mice are infected with HSV-1 in the cornea, and interventions are topically applied at the site of infection to test efficacy. Using standard practice, we infected mice with HSV-1 IE175-YFP, then 6 hours later (to avoid interfering with virus uptake), oligonucleotides were applied and after two days, corneas were harvested for imaging and quantification of viral replication by q-PCR and titering (Fig. 4A). C-DOT uptake by cells was quantified by Cy3 fluorescence (fig. S16A) and as predicted, C-DOT treatment first caused an increase in IE175 (fig. S16B) followed by a significant reduction in the percentage of HSV-1 infected cells (Fig. 4B–C). In agreement with these data, C-DOT^H treatment reduced viral titer by 150-fold (Fig. 4D) and significantly reduced viral genome replication (Fig. 4E). Together, these results demonstrate that feedback disruption reduces viral replication *in vivo*.

Overall, these results indicate that transcriptional feedback could represent a new antiviral target with the potential to substantially delay the emergence of resistance (Fig. 3) and overcome significant treatment barriers including the reduction-in-efficacy at high-viremic loads (26). In general, oligonucleotide therapies offer specificity with the potential for fewer off target effects over small molecules. Delivery of oligonucleotides remains a major challenge but significant clinical advances have been made with the recent FDA approval of antisense and exon-skipping oligonucleotide therapies delivered via nanoparticles (30-32). We also tested C-DOTs using nanoparticle carriers, in the absence of transfection, and found similar antiviral effects (fig. S17). One could envision nanoparticles harboring combinatorial C-DOTs to treat infections of unknown etiology—a significant problem for ocular infections (33, 34). Our data indicate that such combinatorial C-DOTs may be feasible (fig. S18).

From the perspective of resistance, disrupting transcriptional feedback limits escape mutations by reducing the potential of generation of mutants and their selection. First, the IE region has a far lower μ than TK (6, 35) such that mutants in the IE promoter and IE coding regions will arise slowly. Second, our assumption that mutants arise at $\sim\mu^2$ is maximally conservative and based on two single-base mutations being sufficient to recapitulate feedback—one mutation in the promoter to generate a new binding sequence for the new IE protein and one mutation in the protein to generate a new recognition domain to bind the new DNA site. It is likely that > 2 mutations will be required for a new protein recognition domain. So, escape mutants will likely arise at the far slower rate of $\sim\mu^n$ (where $n > 2$). For CMV, with an average $\mu \sim 10^{-4}$ (7) this translates to feedback-disruptor escape mutants arising slower than $\sim 10^{-4n}$ (assuming the IE region follows the average mutation frequency, whereas IE mutation frequency is in fact lower). Regarding selection, the single mutants that do not recapitulate feedback—likely prerequisites for the multiple mutants—have no selective advantage in the presence (or absence) of feedback disruptors. Moreover, prior to feedback disruption, putative C-DOT escape mutants (with perfect feedback recapitulation) would have a relative fitness roughly equivalent to wild type, so their selection coefficient will be small (far lower than for TK mutants $s_{C\text{-DOT}} \ll s_{TK}$) and their arisal time slow. Consequently, the calculations above (Fig. 1C) represent an extreme lower limit for the time to escape from feedback disruptors. We predict that this proof-of-principle based on transcription disruption in herpesviruses could be extended to other viruses, microbes, and even aberrant transcriptional auto-regulatory circuits in neoplastic cells.

References and notes

1. S. Meylan, I. W. Andrews, J. J. Collins, Targeting Antibiotic Tolerance, Pathogen by Pathogen. *Cell* **172**, 1228-1238 (2018).
2. H. H. Lee, M. N. Molla, C. R. Cantor, J. J. Collins, Bacterial charity work leads to population-wide resistance. *Nature* **467**, 82-85 (2010).
3. D. E. Goldberg, R. F. Siliciano, W. R. Jacobs, Jr., Outwitting evolution: fighting drug-resistant TB, malaria, and HIV. *Cell* **148**, 1271-1283 (2012).
4. A. S. Perelson, Modelling viral and immune system dynamics. *Nat Rev Immunol* **2**, 28-36 (2002).
5. J. M. Coffin, HIV population dynamics in vivo: implications for genetic variation, pathogenesis, and therapy. *Science* **267**, 483-489 (1995).
6. Q. Lu, Y. T. Hwang, C. B. Hwang, Mutation spectra of herpes simplex virus type 1 thymidine kinase mutants. *J Virol* **76**, 5822-5828 (2002).
7. N. Renzette, B. Bhattacharjee, J. D. Jensen, L. Gibson, T. F. Kowalik, Extensive genome-wide variability of human cytomegalovirus in congenitally infected infants. *PLoS Pathog* **7**, e1001344 (2011).
8. J. Piret, G. Boivin, Antiviral drug resistance in herpesviruses other than cytomegalovirus. *Rev Med Virol* **24**, 186-218 (2014).
9. N. S. Lurain, S. Chou, Antiviral drug resistance of human cytomegalovirus. *Clin Microbiol Rev* **23**, 689-712 (2010).
10. E. Frobert *et al.*, Resistance of herpes simplex viruses to acyclovir: an update from a ten-year survey in France. *Antiviral Res* **111**, 36-41 (2014).
11. V. C. Emery, P. D. Griffiths, Prediction of cytomegalovirus load and resistance patterns after antiviral chemotherapy. *Proc Natl Acad Sci U S A* **97**, 8039-8044 (2000).
12. D. M. Coen, P. A. Schaffer, Two distinct loci confer resistance to acycloguanosine in herpes simplex virus type 1. *Proc Natl Acad Sci U S A* **77**, 2265-2269 (1980).
13. T. Goldner *et al.*, The novel anticytomegalovirus compound AIC246 (Letermovir) inhibits human cytomegalovirus replication through a specific antiviral mechanism that involves the viral terminase. *J Virol* **85**, 10884-10893 (2011).
14. D. Jaishankar *et al.*, An off-target effect of BX795 blocks herpes simplex virus type 1 infection of the eye. *Sci Transl Med* **10**, (2018).
15. A. Pai, L. S. Weinberger, Fate-Regulating Circuits in Viruses: From Discovery to New Therapy Targets. *Annu Rev Virol* **4**, 469-490 (2017).
16. L. W. Enquist, D. A. Leib, Intrinsic and Innate Defenses of Neurons: Detente with the Herpesviruses. *J Virol* **91**, (2017).
17. S. K. Weller, D. M. Coen, Herpes simplex viruses: mechanisms of DNA replication. *Cold Spring Harb Perspect Biol* **4**, a013011 (2012).
18. T. E. Shenk, M. F. Stinski, Human cytomegalovirus. Preface. *Curr Top Microbiol Immunol* **325**, v (2008).
19. E. S. Mocarski, T. Shenk, R. F. Pass, in *Fields' virology*, D. M. Knipe, Ed. (Lippincott Williams & Wilkins, Philadelphia, 2006), pp. 2708-2772.
20. B. Liu, T. W. Hermiston, M. F. Stinski, A cis-acting element in the major immediate-early (IE) promoter of human cytomegalovirus is required for negative regulation by IE2. *J Virol* **65**, 897-903 (1991).

21. T. Paterson, R. D. Everett, The regions of the herpes simplex virus type 1 immediate early protein Vmw175 required for site specific DNA binding closely correspond to those involved in transcriptional regulation. *Nucleic Acids Res* **16**, 11005-11025 (1988).
22. M. W. Teng *et al.*, An endogenous accelerator for viral gene expression confers a fitness advantage. *Cell* **151**, 1569-1580 (2012).
23. H. Isomura *et al.*, A cis element between the TATA Box and the transcription start site of the major immediate-early promoter of human cytomegalovirus determines efficiency of viral replication. *J Virol* **82**, 849-858 (2008).
24. N. Vardi, S. Chaturvedi, L. S. Weinberger, Feedback-mediated signal conversion promotes viral fitness. *Proc Natl Acad Sci U S A* **115**, E8803-E8810 (2018).
25. R. D. Everett, J. Murray, A. Orr, C. M. Preston, Herpes simplex virus type 1 genomes are associated with ND10 nuclear substructures in quiescently infected human fibroblasts. *J Virol* **81**, 10991-11004 (2007).
26. A. Asberg *et al.*, Lessons Learned From a Randomized Study of Oral Valganciclovir Versus Parenteral Ganciclovir Treatment of Cytomegalovirus Disease in Solid Organ Transplant Recipients: The VICTOR Trial. *Clin Infect Dis* **62**, 1154-1160 (2016).
27. S. Luecke *et al.*, cGAS is activated by DNA in a length-dependent manner. *EMBO Rep* **18**, 1707-1715 (2017).
28. G. B. Mulamba, A. Hu, R. F. Azad, K. P. Anderson, D. M. Coen, Human cytomegalovirus mutant with sequence-dependent resistance to the phosphorothioate oligonucleotide fomivirsen (ISIS 2922). *Antimicrob Agents Chemother* **42**, 971-973 (1998).
29. S. Lahmidi, M. Yousefi, S. Dridi, P. Duplay, A. Pearson, Dok-1 and Dok-2 Are Required To Maintain Herpes Simplex Virus 1-Specific CD8(+) T Cells in a Murine Model of Ocular Infection. *J Virol* **91**, (2017).
30. D. Adams *et al.*, Patisiran, an RNAi Therapeutic, for Hereditary Transthyretin Amyloidosis. *N Engl J Med* **379**, 11-21 (2018).
31. R. Kanasty, J. R. Dorkin, A. Vegas, D. Anderson, Delivery materials for siRNA therapeutics. *Nat Mater* **12**, 967-977 (2013).
32. A. Khvorova, J. K. Watts, The chemical evolution of oligonucleotide therapies of clinical utility. *Nat Biotechnol* **35**, 238-248 (2017).
33. E. T. Cunningham, Cytomegalovirus: ophthalmic perspectives on a pervasive pathogen. *Expert Review of Ophthalmology* **6**, 489-491 (2011).
34. M. H. Elia, J.J., and Gaudio, P.A., in *EyeNet Magazine*. (2016), pp. 37-38.
35. N. Renzette *et al.*, Limits and patterns of cytomegalovirus genomic diversity in humans. *Proc Natl Acad Sci U S A* **112**, E4120-4128 (2015).

Acknowledgments

Acknowledgments: We dedicate the manuscript to the memory of Cynthia-Bolovan-Fritts who provided extensive technical support and made this work possible. We acknowledge Ariel Weinberger and Raghav Singhal for their valuable input in modeling the ACV/GCV resistance. We thank Lewis Lanier, Peter Barry and Roger Everett for kindly providing MCMV strain K181, Rhesus CMV 68.1 EGFP, HSV-1 17syn+ IE175-YFP virus. We would like to thank Melanie Ott, JJ Miranda, Siyu Zheng, Marielle Cavrois and Nandani Raman for valuable discussions and technical expertise, and Elizabeth Tanner and rest of the members of Weinberger lab for thoughtful discussions and valuable suggestions. We thank Kathryn Claiborn for reviewing the manuscript. Gladstone Flow Cytometry Core, funded through NIH P30 AI027763.

Funding: L.S.W. acknowledges support from the Bowes Distinguished Professorship, the Alfred P. Sloan Research Fellowship, NIH Director's New Innovator Award OD006677 and Pioneer Award OD17181 programs.

Author contributions: S.C and L.S.W conceived and designed the study. S.C, M.W, and M.C, designed and performed the experiments, and curated the data. N.V., A.D.W, R.S, and L.S.W. performed the mathematical modeling. S.C, M.W and L.S.W wrote the paper.

Competing interests: L.S.W. is a co-founder of Autonomous Therapeutics Inc. and serves as chair of its Scientific Advisory Board.

Data and materials availability: NA

Supplementary Materials:

Materials and Methods

Tables S1-S2

Figure legends

Figures S1-S18

FIGURE LEGENDS:

Figure 1: Theory predicts that antiviral disruption of transcriptional feedback would substantially delay evolution of resistance. (A) Schematics of the herpesvirus IE (IE86 and IE175) transcriptional negative-feedback circuits in the intact wild-type form (upper) and after disruption (lower) by putative circuit-disrupting oligonucleotide therapy (C-DOT). When feedback is intact, IE proteins bind the cis repression DNA sequence in their respective IE promoters (cyan) and downregulate transcriptional activity to prevent IE protein levels from reaching cytotoxic levels. When feedback is disrupted, for example by IE proteins being titrated away by binding free oligonucleotides encoding cis-repression sequences, IE promoter activity is not downregulated and IE proteins reach cytotoxic levels (~1.5-fold above homeostatic levels). (B) Numerical solutions of an experimentally validated computational model of IE feedback (22, 24) showing that C-DOTs effectively break feedback to increase IE protein levels into the cytotoxic regime. See also fig. S1. (C) Analytical calculation for the 50% emergence time of resistance mutants ($\tau_{\text{resistance}}$) as a function of the mutation rate μ . The observed emergence of resistance to GCV in the clinic (11) is shown as a point above the measured TK mutation rate ($\mu = 10^{-4}$). Putative C-DOT resistance, predicted to require at least two mutations (one in the protein and one in the promoter), is shown as a line corresponding to measured μ (7). Inset: representative dynamics of emergence for either a GCV mutant (black) or a putative C-DOT mutant (cyan) that requires only viral two mutations. See Methods for equations..

Figure 2: Biochemical and *in vitro* analyses identify oligonucleotides that disrupt transcriptional feedback circuitry. (A) Schematic of the IE86-protein binding assay: the C-terminus of the IE86 protein was expressed in *E. coli*, concentrated and incubated with 14–64bp DNA oligonucleotides for 30 minutes at room temperature, then passed through an FPLC column. Protein-DNA complex formation was quantified by optical density (OD 280nm) of FPLC fractions; the IE86 protein (obligate dimer) fragment elutes in the 15mL fraction, free dsDNA oligonucleotides elute in the 18mL fraction, and the multimeric protein-DNA complex elutes in the 13mL fraction. (B) FPLC chromatography profiles of IE86 protein fragment input and dsDNA input prior to co-incubation. (C) Chromatographs of IE86 fragment incubated with either a sequence-scrambled control dsDNA oligonucleotides or crs-containing dsDNA oligonucleotides of differential lengths. The 28bp crs DNA oligonucleotide most efficiently titrates free protein from the 15mL fraction into the 13mL fraction (~98% of protein is found in the 13mL protein-DNA complex fraction when the 28bp crs DNA oligonucleotide is added). (D) Left: Schematic of the minimal IE negative-feedback circuit (MIEP-IE86-IRES-GFP) encoded within the feedback-reporter cell line. Disruption of negative feedback generates increases in GFP fluorescence. Right: Flow cytometry of feedback reporter cells 48 h after nucleofection with either a 28bp crs-containing DNA oligonucleotide, a scrambled DNA oligonucleotide (negative control), or mock nucleofection (no DNA oligonucleotide) showing that crs-encoding DNA oligonucleotides disrupt feedback and act as a putative C-DOTs. (E, F) The 28bp crs-containing DNA oligonucleotide optimally disrupts feedback and induces cytotoxicity in the feedback-reporter cell line. DNA oligonucleotides (from the FPLC analysis in panel C above) were nucleofected into the reporter cell line and analyzed by flow cytometry after 48 h to determine IE86 expression (GFP; panel E),

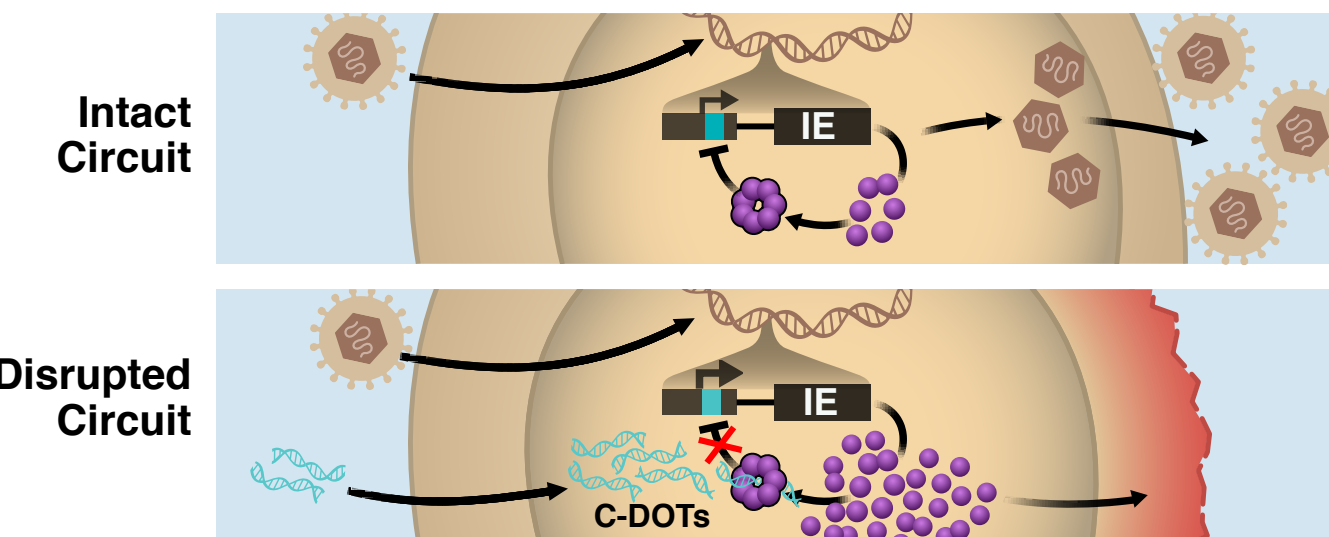
and cytotoxicity (panel F). (p-value less than 0.05 was considered statistically significant: * <0.05 , ** <0.01 , *** <0.001 , **** <0.0001).

Figure 3: Feedback circuit disruption interferes with viral replication even at high MOI and limits the evolution of resistance. (A) Flow cytometry of ARPE-19 cells nucleofected with the 28bp dsDNA that titrates IE86 (C-DOT^C) or scrambled dsDNA sequence (C-DOT^{Scram}) and infected with a clinically derived CMV (TB40E) encoding an IE86-YFP (MOI = 0.1) then analyzed at 2 days post infection (dpi). (B) Flow cytometry of ARPE-19 cells nucleofected with a 29bp DNA to titrate IE175 (C-DOT^H) or scrambled dsDNA sequence (C-DOT^{Scram}) and infected with HSV-1 (17syn+ strain) encoding an IE175-YFP (MOI = 0.1) then analyzed at 2 dpi. (C) Single-round viral titering of CMV in the presence of 100 μ M GCV, PBS, or 25 μ M C-DOT^C (or C-DOT^{Scram}) at 4-days post infection under different initial MOIs. (D) Single-round viral titering of HSV-1 in presence of 100 μ M ACV or 25 μ M C-DOT^H (or C-DOT^{Scram}) at 4-days post infection under different HSV-1 MOIs. (E) Schematic of the continuous-culture experiment; ARPE-19 cells (+/- C-DOT) were infected with CMV or HSV-1 (0.1 MOI) and at 4-day post infection, supernatant was collected and was used to infect naïve ARPE-19 cells +/- C-DOT until day 60. (F) Continuous culture titers for CMV (TB40E-IE86-YFP) in the presence of C-DOT^C (red) or mock treatment (black). Fomivirsen resistance (positive slope of the titering dynamics) was observed beginning at day 12 (fig. S11A-B). (G) Continuous culture for HSV-1 (17syn+ IE175-YFP virus) in the presence of C-DOT^H (red) or mock treatment (black). ACV resistance (positive slope of the titering dynamics) observed beginning at day 4 (fig. S11C).

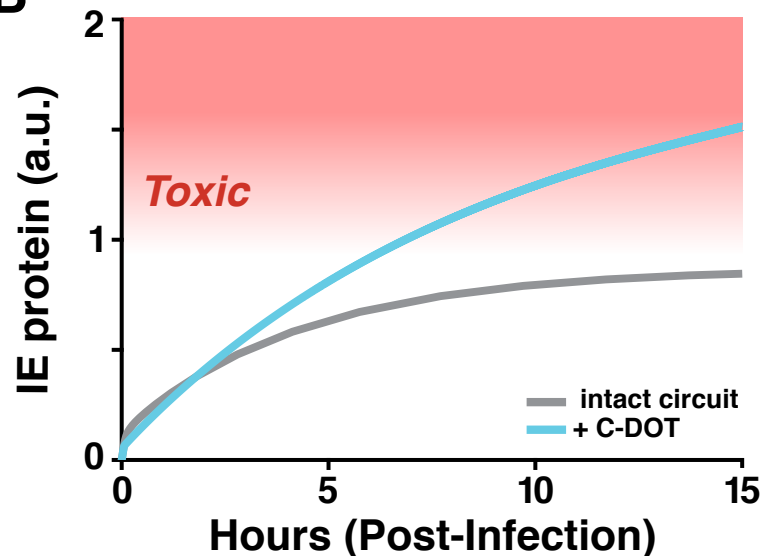
Figure 4: Feedback disruption inhibits viral replication in an *in vivo* model. (A) Schematic of the HSV-1 corneal infection model in mice. BL-6 mice, 6-10 weeks old, undergo corneal debridement followed by infection with HSV-1 17syn+ IE175-YFP virus (1×10^5 PFU). 6 hours post infection, 25 μ M C-DOT^H, or C-DOT^{Scram}, or PBS, was topically applied to the cornea. Corneas were harvested at 2 days post infection, imaged for YFP, HSV-1 levels quantified by virus titering, and viral genomes quantified by qPCR. (B) Representative YFP-fluorescence images of corneas after harvesting (nuclei stained with DAPI). (C) Quantification of HSV-1 YFP expressing cells in corneas, as determined from the YFP:DAPI ratio. 5 corneas imaged per sample. (D) HSV-1 viral titers from HSV-1 infected corneas 2 days after treatment with either 25 μ M PBS, C-DOT^{Scram} or C-DOT^H. Corneas were dissociated using collagenase, subjected to three freeze-thaw and supernatant was used to titer virus using end time dilution method (TCID50). Each data point represents a pooling of corneas from three mice (i.e., 9 corneas per treatment). (E) HSV-1 viral genomic DNA quantification by qPCR 2 days after treatment. Each data point represents a pooling of corneas from three mice (i.e., 9 corneas per treatment). p-values less than 0.05 were considered statistically significant: * <0.05 , ** <0.01 , *** <0.001 .

Figure 1 (Chaturvedi et.al)

A



B



C

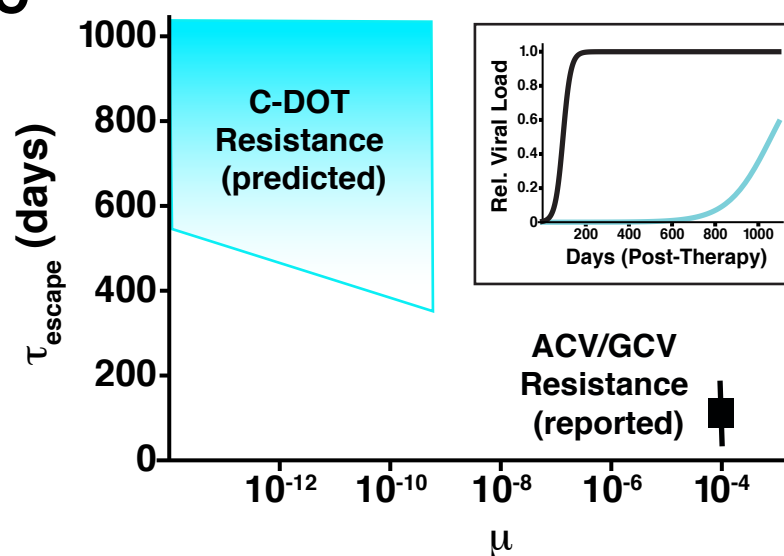


Figure 2 (Chaturvedi et.al)

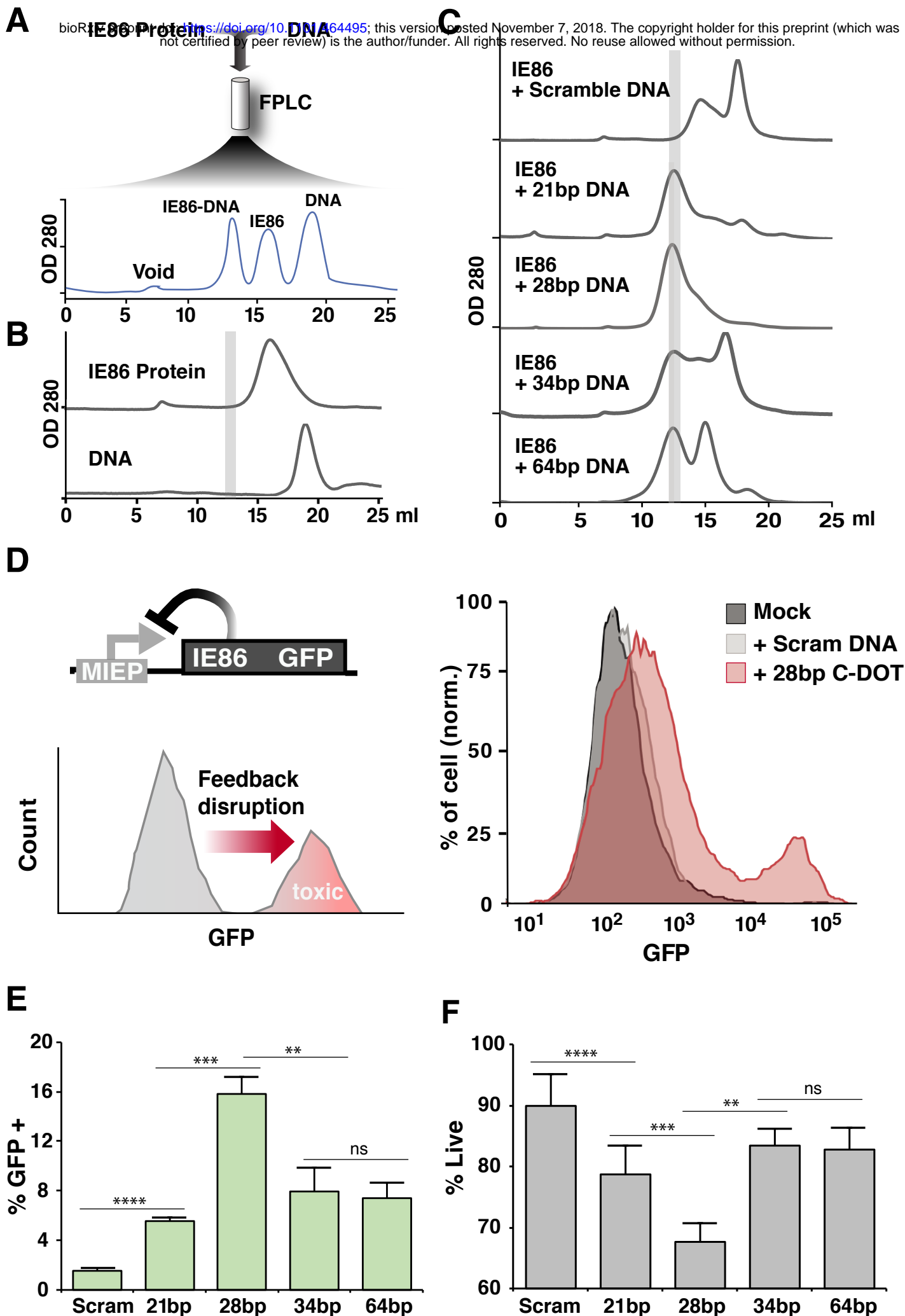


Figure 3 (Chaturvedi et al.)

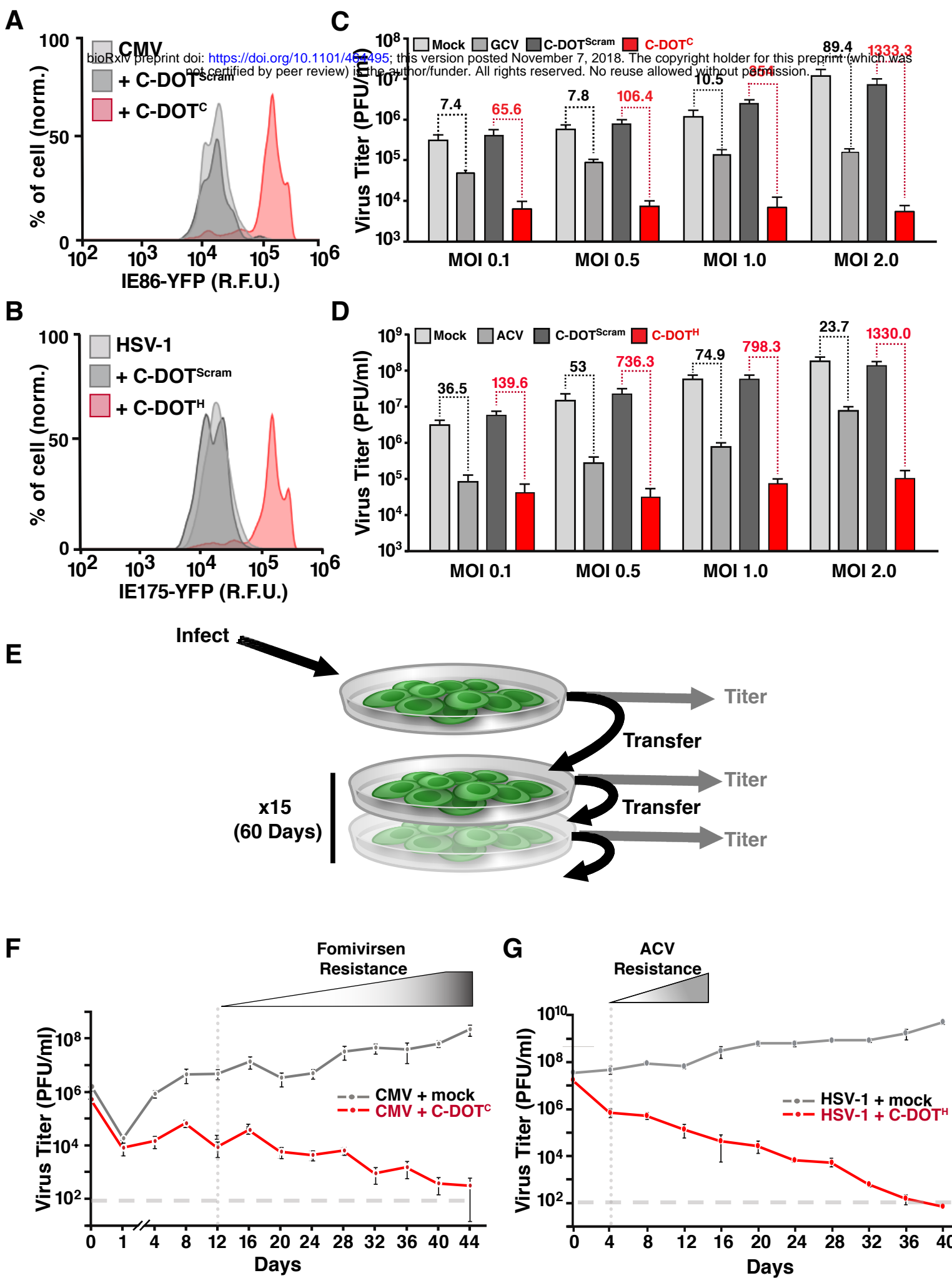


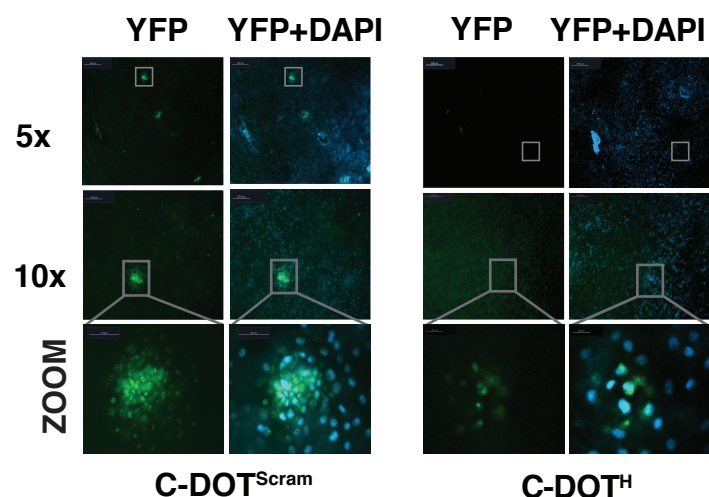
Figure 4 (Chaturvedi et al.)

bioRxiv preprint doi: <https://doi.org/10.1101/464495>; this version posted November 7, 2018. The copyright holder for this preprint (which was not certified by peer review) is the author/funder. All rights reserved. No reuse allowed without permission.

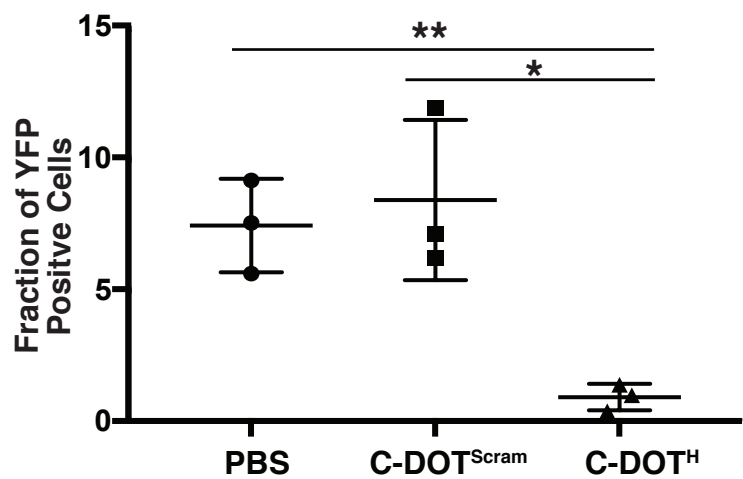
A



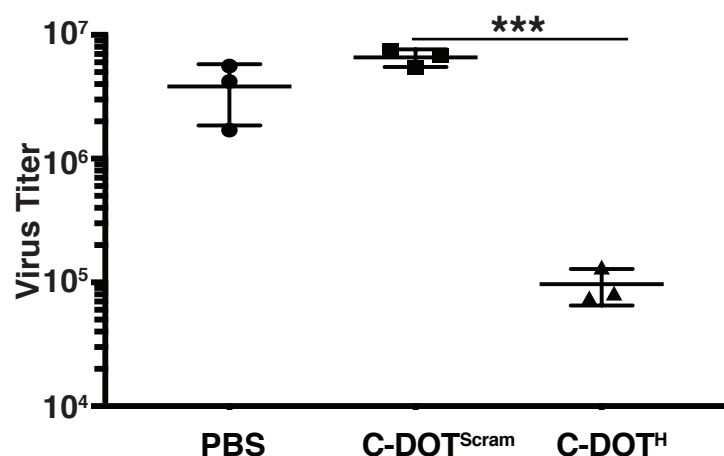
B



C



D



E

